

**Title: Electron transport through a (terpyridine)ruthenium metallosurfactant containing a redox-active aminocatechol derivative**

Samudra Amunugama, Eyram Asempa, Ramesh Chandra Tripathi, Dakshika Wanniarachchi, Habib Baydoun, Peter Hoffman, Elena Jakubikova and Cláudio N. Verani

**Outline**

**Figure S1.**  $^1\text{H}$ -NMR spectrum of 4'-(4-(octadecyloxy)phenyl)-2,2':6'2''-terpyridine ( $\text{L}^{\text{terpy}}$ ) ligand

**Figure S2.**  $^1\text{H}$ -NMR spectrum of 3,5-ditert-butyl-2-(phenylamino)catechol ( $\text{L}^2\text{H}_2$ ) ligand

**Figure S3.** Full  $^1\text{H}$ -NMR spectrum of  $[\text{Ru}(\text{L}^{\text{terpy}})(\text{L}^2)\text{Cl}] \text{PF}_6$  **1**

**Figure S4.**  $^{13}\text{C}$ -NMR spectrum of  $[\text{Ru}(\text{L}^{\text{terpy}})(\text{L}^2)\text{Cl}] \text{PF}_6$  **1**

**Figure S5.** HSQC NMR spectrum of  $[\text{Ru}(\text{L}^{\text{terpy}})(\text{L}^2)\text{Cl}] \text{PF}_6$  **1**

**Figure S6.** Crystal structure of complex **1** with 50% probability

**Figure S7:** UV-visible spectrum of complex **1** in dichloromethane. Inset shows the magnification of 600-1600 nm region of the UV-visible spectrum

**Table T1.** Crystal structure data and selected bond lengths for complex **1**

**Table T2.** Electrochemical data recorded in dichloromethane for complex **1**

**Figure S8.** Triplicate measurements of isothermal compression for  $[\text{Ru}(\text{L}^{\text{terpy}})(\text{L}^2)\text{Cl}] \text{PF}_6$  **1**

**Figure S9.** Comparison of IRRAS spectrum of 57 layers of LB film and IR spectrum of  $[\text{Ru}(\text{L}^{\text{terpy}})(\text{L}^2)\text{Cl}] \text{PF}_6$  **1**

**Figure S10.** Comparison of UV-vis spectrum of 57 layers of LB film and solution state UV-vis spectrum of  $[\text{Ru}(\text{L}^{\text{terpy}})(\text{L}^2)\text{Cl}] \text{PF}_6$  **1** (b) Mass spectrum of **1** recovered from LB films

**Figure S11.** AFM height images for 9-monolayers of complex **1** deposited on quartz substrate (a) 3D view (b) sectional analysis

**Figure S12.** Geometric parameters for  $[\text{Ru}(\text{L}^{\text{terpy}})(\text{L}^2)\text{Cl}] \text{PF}_6$  **1** coordination environment

**Table T3.** Metal-ligand bond lengths for singlet, triplet, quintet, and septet states of the Ru complex optimized at the B3LYP+D3/SDD,6-311G\* level of theory as well as crystal structure data. The values in parentheses correspond to the optimized values in dichloromethane (PCM solvent model).

**Table T4.** Energetics for singlet, triplet, quintet, and septet states of Complex **1** in dichloromethane (PCM solvent model)

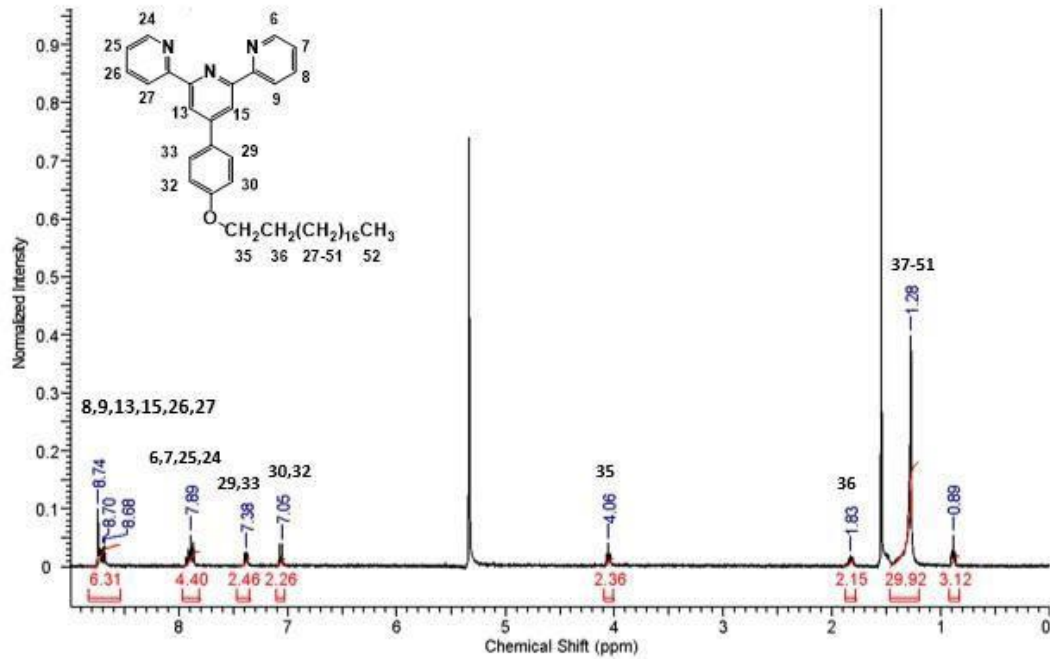
**Figure S13.** Calculated absorption spectrum with corresponding stick spectrum of  $[\text{Ru}(\text{L}^{\text{terpy}})(\text{L}^2)\text{Cl}] \text{PF}_6$  **1**

**Table T5.** Calculated Electrochemical data for Ru aminocatechol in dichloromethane (PCM solvent model)

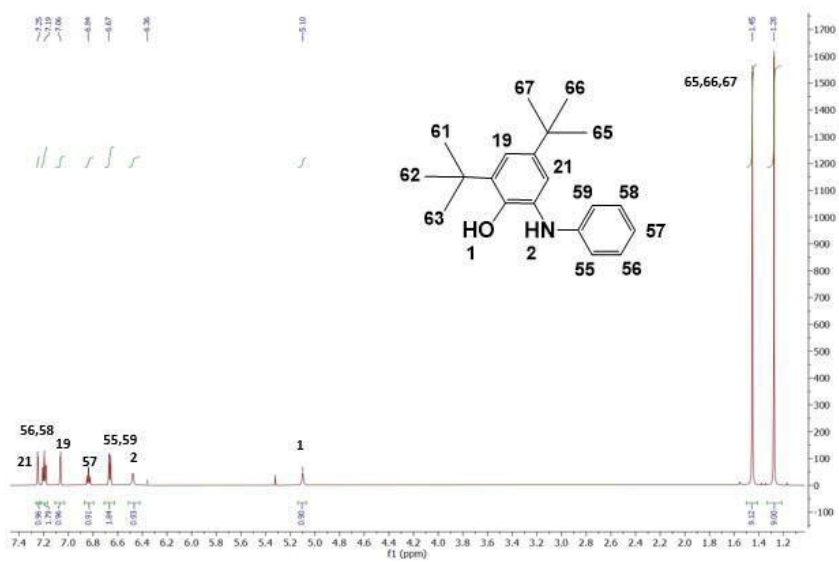
**Figure S14.** Singly-occupied natural orbitals of the oxidized and reduced species of  $[\text{Ru}(\text{L}^{\text{terpy}})(\text{L}^2)\text{Cl}] \text{PF}_6$  **1** in dichloromethane

**Figure S15.** I-V characteristics for  $[\text{Ru}(\text{L}^{\text{terpy}})(\text{L}^2)\text{Cl}] \text{PF}_6$  **1** in five devices

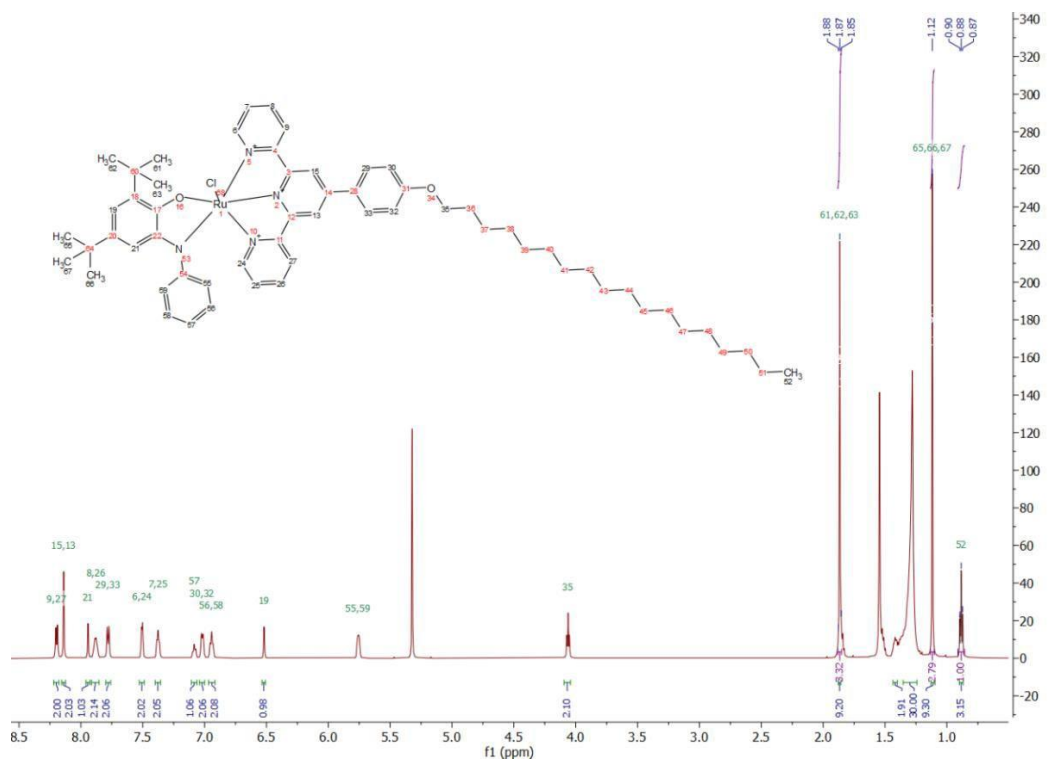
**Figure S1:**  $^1\text{H}$ -NMR spectrum of 4'-(4-(octadecyloxy)phenyl)-2,2':6'2''-terpyridine ( $\text{L}^{\text{terpy}}$ ) ligand



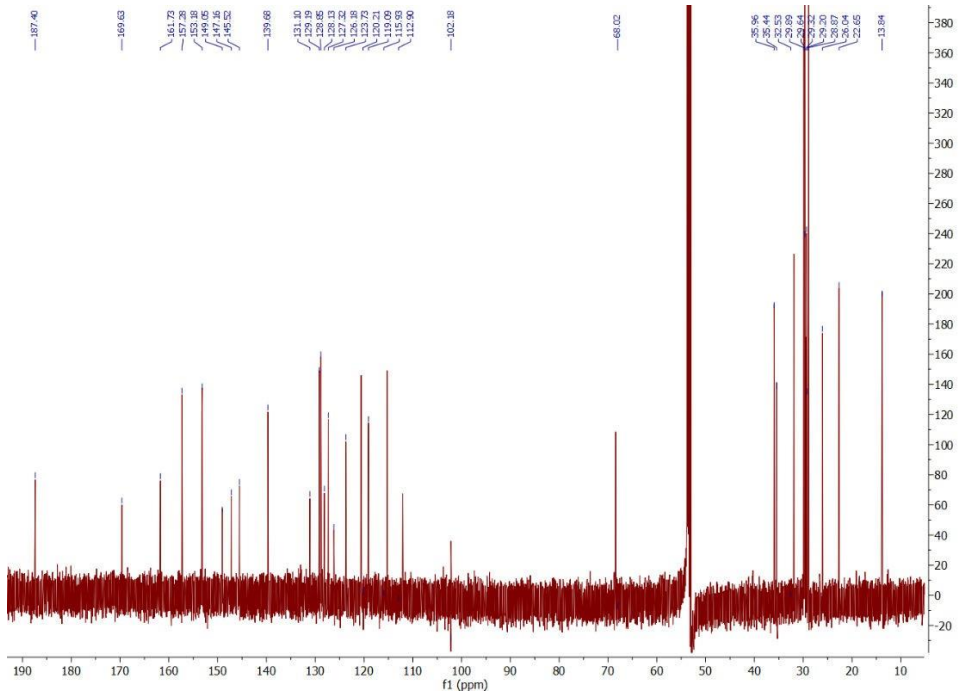
**Figure S2:**  $^1\text{H}$ -NMR spectrum of 3,5-ditert-butyl-2-(phenylamino)catechol ( $\text{L}^2\text{H}_2$ ) ligand



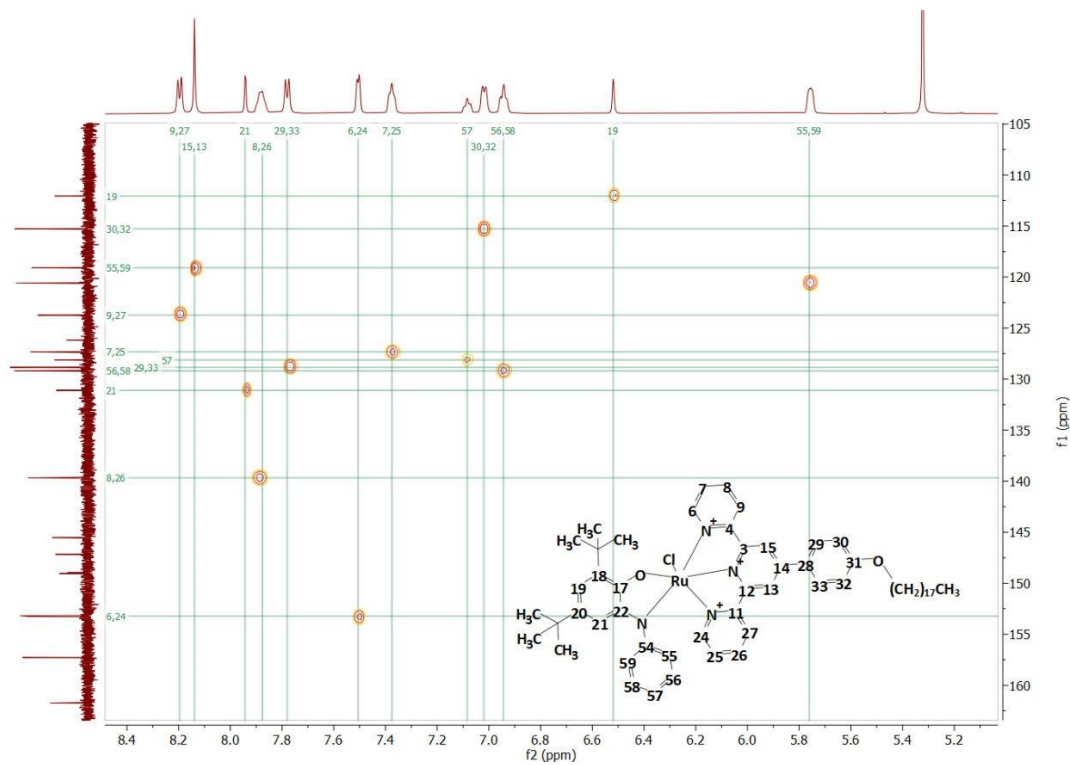
**Figure S3:** Full  $^1\text{H}$ -NMR spectrum of  $[\text{Ru}(\text{L}^{\text{terpy}})(\text{L}^2)\text{Cl}]\text{PF}_6$  **1**



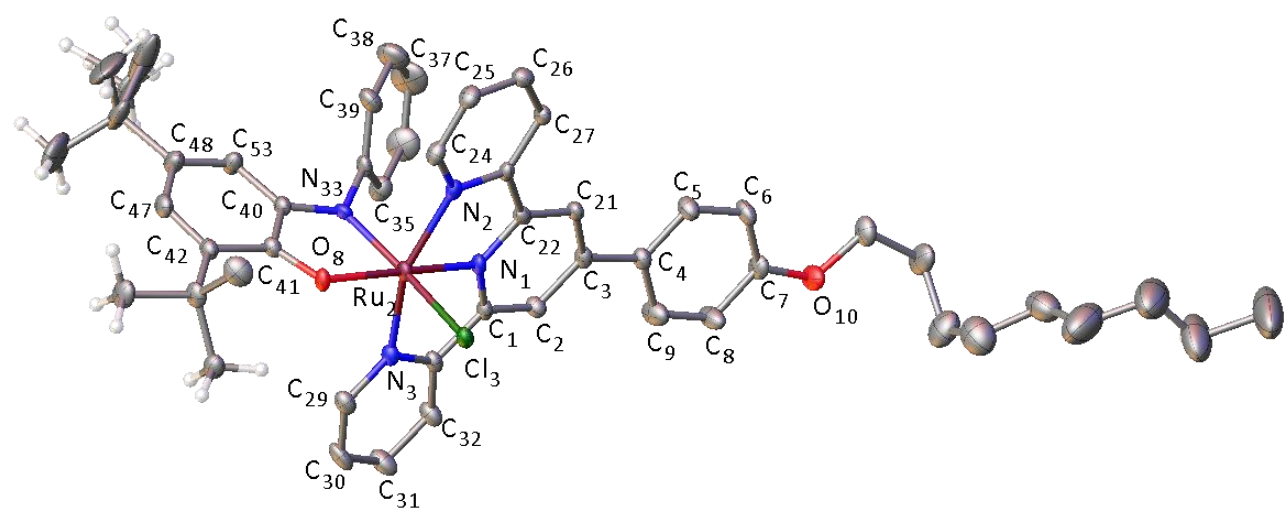
**Figure S4:**  $^{13}\text{C}\{^1\text{H}\}$  NMR spectrum of  $[\text{Ru}(\text{L}^{\text{terpy}})(\text{L}^2)\text{Cl}]\text{PF}_6$  **1**



**Figure S5:** HSQC NMR spectrum of  $[\text{Ru}(\text{L}^{\text{terpy}})(\text{L}^2)\text{Cl}] \text{PF}_6$  **1**



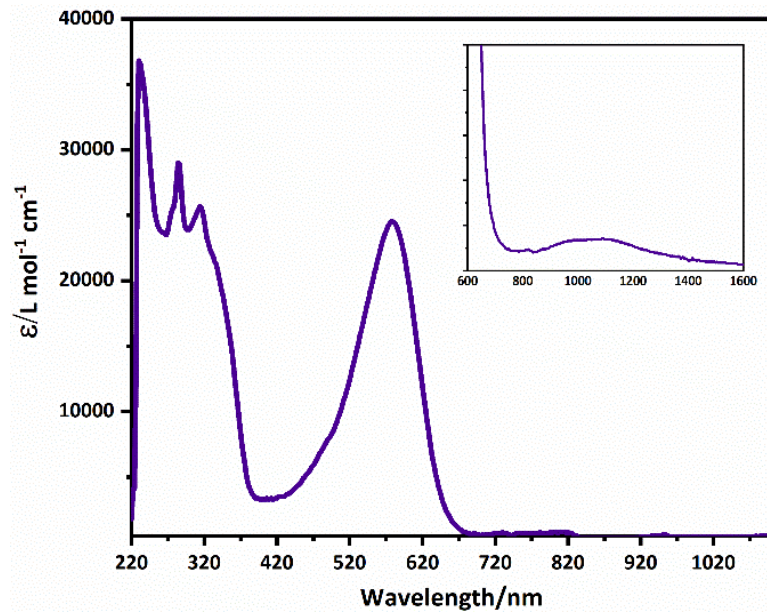
**Figure S6:** Crystal structure of complex **1** with 50% probability



**Table T1:** Crystal structure data and selected bond lengths for complex **1**

	<b>1</b>		<b>Bond length(Å°)</b>	<b>1</b>
Formula	C <sub>57</sub> H <sub>64.7</sub> ClF <sub>6</sub> N <sub>4</sub> O <sub>2</sub> PRu		Ru-N1	1.972(2)
FW	1157.66		Ru-N2	2.073(3)
Space group	P-1		Ru-N3	2.068(2)
a(Å°)	12.8026(6)		Ru-O8	2.0365(19)
b(Å°)	15.0623(8)		Ru-N33	1.971(2)
c(Å°)	19.8264(10)		Ru-Cl	2.3875(7)
α(deg)	68.182(3)		C40-N33	1.347
β(deg)	88.474(3)		C41-O8	1.281
γ(deg)	66.262(3)		C40-C41	1.444
V(Å°) <sup>3</sup>	3214.9(3)		C41-C42	1.443
Z	2		C42-C47	1.362
Temp(K)	100		C47-C48	1.438
λ(Å°)	0.71073		C48-C53	1.366
ρ(g m <sup>-3</sup> )	1.196		C53-C40	1.412
μ(mm <sup>-1</sup> )	0.368		Diameter(C31-C13)	10.244
R(F)(%)	5.60		Area(Å°) <sup>2</sup> (Circular)	82.45
Rw(F)(%)	14.2		Volume	2042
			Length (C46-C10)	24.768

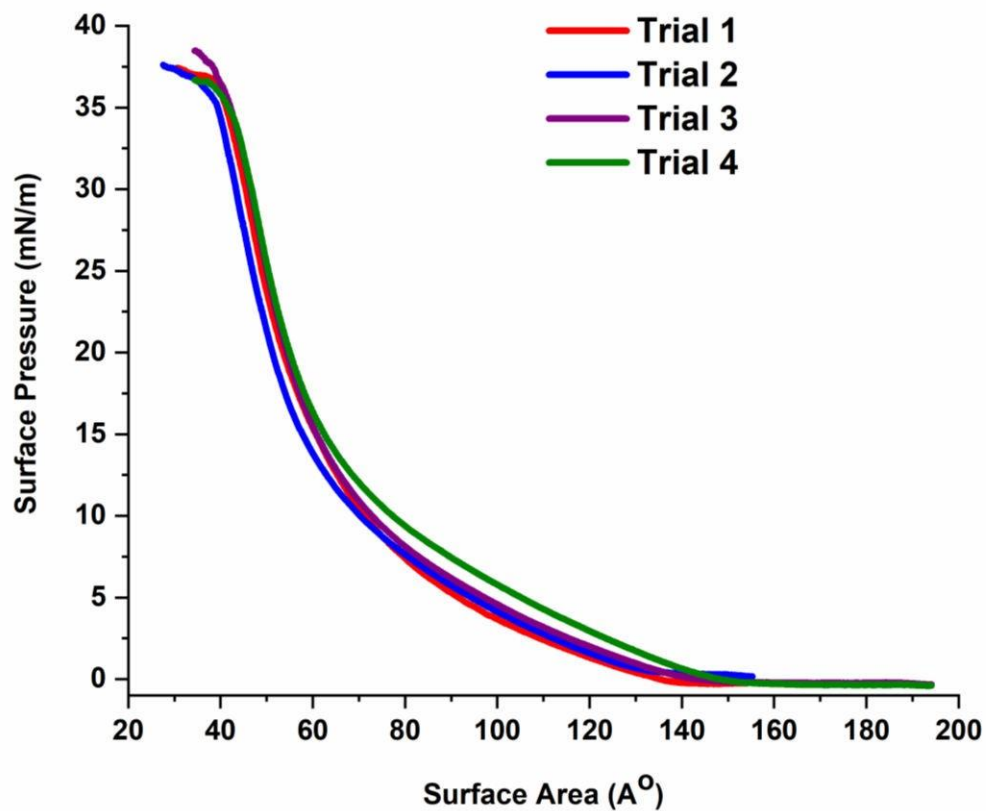
**Figure S7:** UV-visible spectrum of complex **1** in dichloromethane. Inset shows the magnification of 600-1600 nm region of the UV-visible spectrum



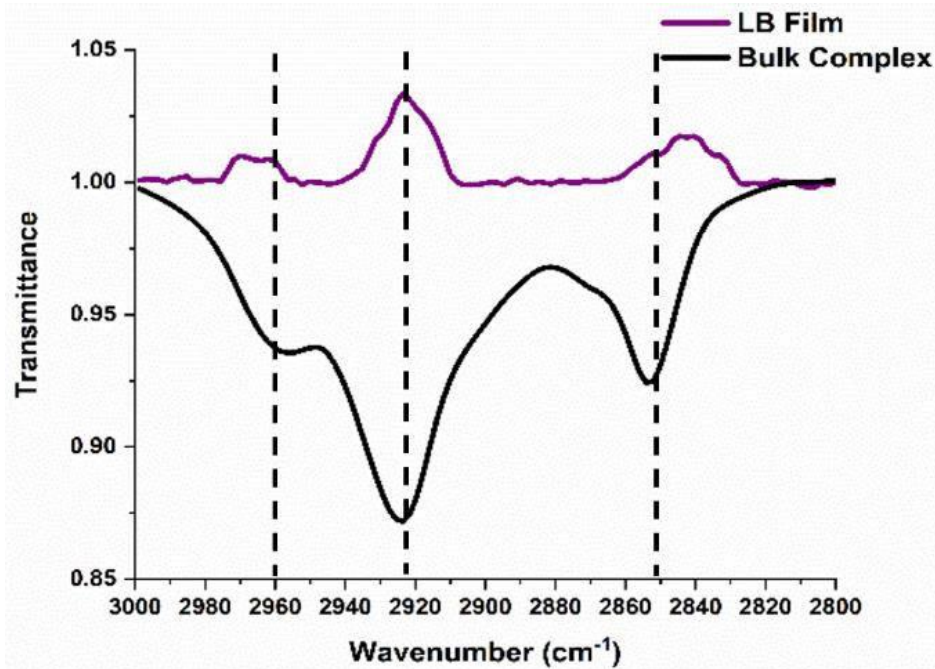
**Table T2:** Electrochemical data recorded in dichloromethane for complex **1**

Peak Assignment	$E_{1/2}(\Delta E_P)/V$ $ I_{pa}/I_{pc} $			
<b>Complex 1</b>	<b>0.76 (90)</b> <b> 1.18 </b>	<b>-0.76 (72)</b> <b> 0.95 </b>	<b>-1.60 (74)</b> <b> 1.11 </b>	<b>-2.20</b>

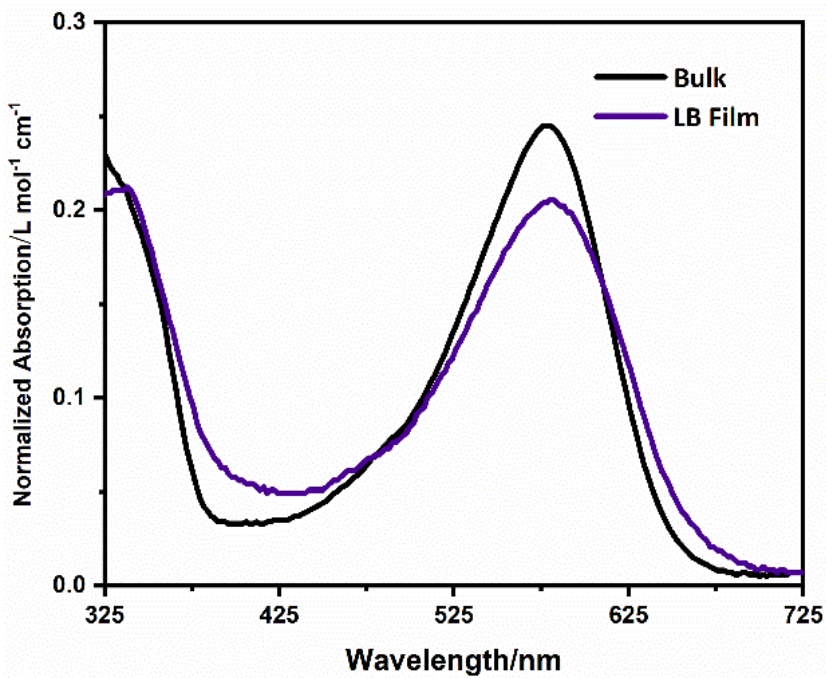
**Figure S8:** Triplicate measurements of isothermal compression for  $[\text{Ru}(\text{L}^{\text{terpy}})(\text{L}^2)\text{Cl}]\text{PF}_6$  **1**



**Figure S9:** Comparison of IRRAS spectrum of 57 layers of LB film and IR spectrum of  $[\text{Ru}(\text{L}^{\text{terpy}})(\text{L}^2)\text{Cl}]\text{PF}_6$  **1**



**Figure S10:** (a) Comparison of UV-vis spectrum of 57 layers of LB film and solution state UV-vis spectrum of complex **1** (b) Mass spectrum of **1** recovered from LB films



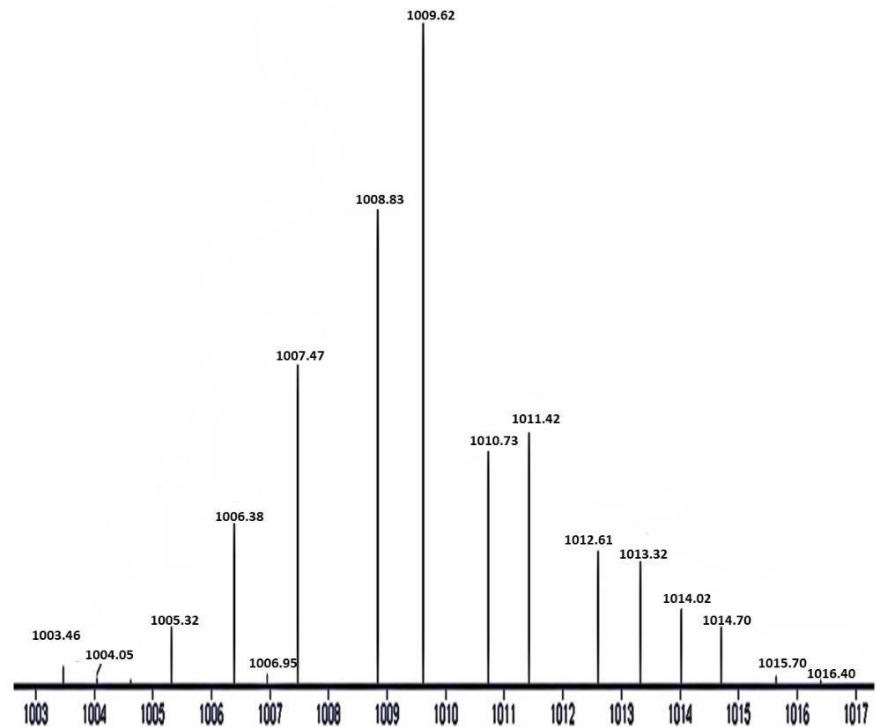


**Figure S11:** AFM height images for 9-monolayers of complex **1** deposited on quartz substrate (a) 3D view (b) sectional analysis

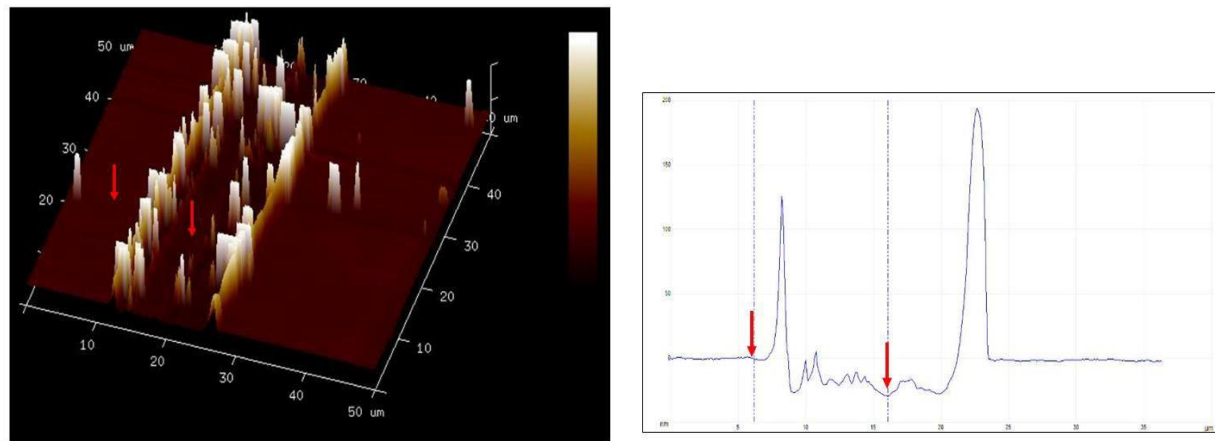


**Figure S12:** Geometric parameters for  $[\text{Ru}(\text{L}^{\text{terpy}})(\text{L}^2)\text{Cl}] \text{PF}_6$  **1** coordination environment

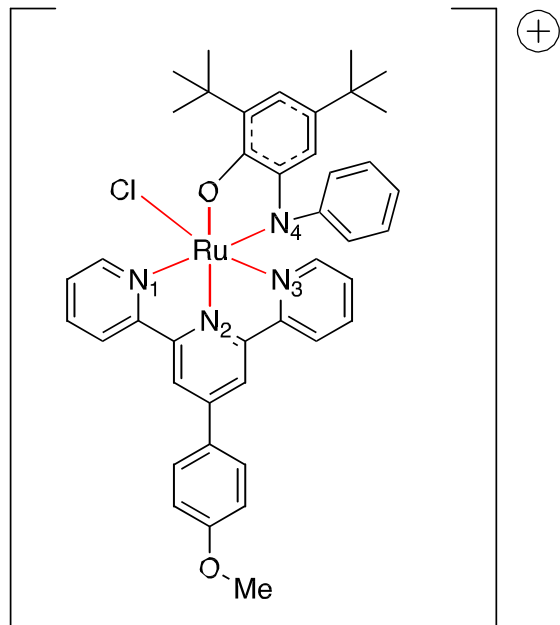


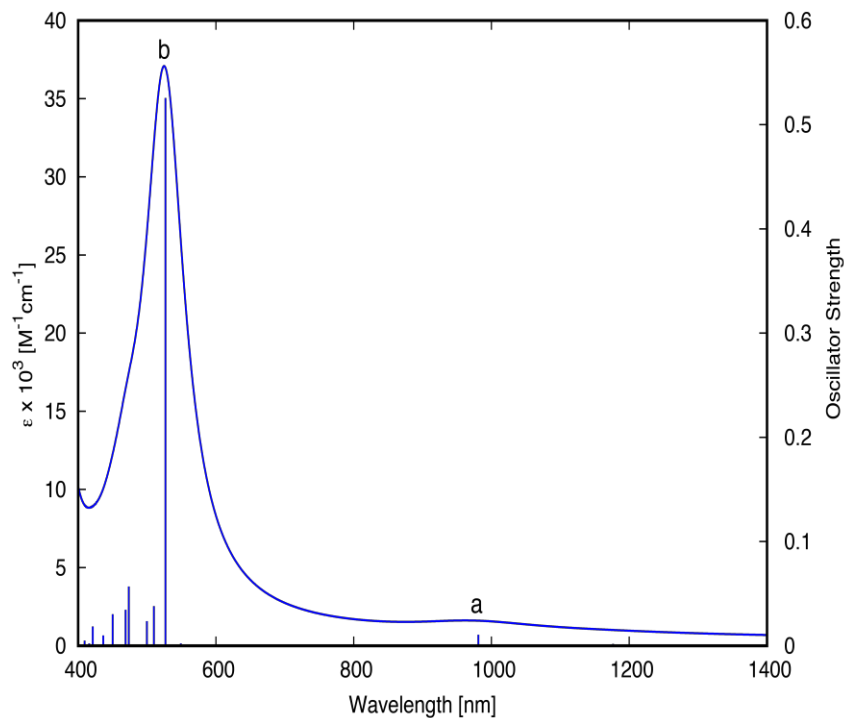
**Table T3:** Metal-ligand bond lengths for singlet, triplet, quintet, and septet states of the Ru complex optimized at the B3LYP+D3/SDD,6-311G\* level of theory as well as crystal structure data. The values in parentheses correspond to the optimized values in dichloromethane (PCM solvent model).

Bond lengths (Å)	Experimental	Singlet	Triplet	Quintet	Septet
Ru-Cl	2.39	2.42	2.39	2.32	2.31
Ru-N <sub>1</sub>	2.07	2.08	2.09	2.08	2.08
Ru-N <sub>2</sub>	1.97	1.97	2.00	1.94	1.95
Ru-N <sub>3</sub>	2.07	2.09	2.08	2.09	2.08
Ru-N <sub>4</sub>	1.97	1.98	2.03	2.05	2.05
Ru-O	2.04	2.07	2.02	2.04	2.03

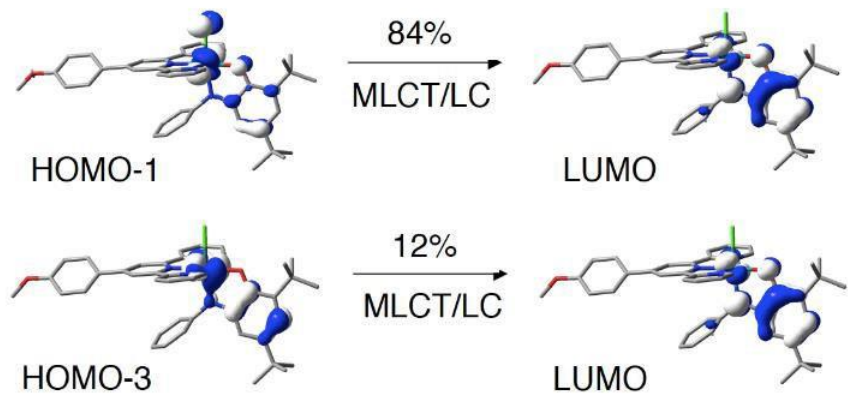
**Table T4:** Energetics for singlet, triplet, quintet, and septet states of Complex **1** in dichloromethane (PCM solvent model)

Spin states	Relative $\Delta E$ (kcal/mol)
Singlet	0.00
Triplet	10.60
Quintet	57.49
Septet	119.02

**Figure S13:** Calculated absorption spectrum with corresponding stick spectrum of  $[\text{Ru}(\text{L}^{\text{terpy}})(\text{L}^2)\text{Cl}]\text{PF}_6$  **1**



A) Excited state 2:  $\lambda = 981$  nm  $f = 0.01$



B) Excited state 4:  $\lambda = 527$  nm  $f = 0.53$

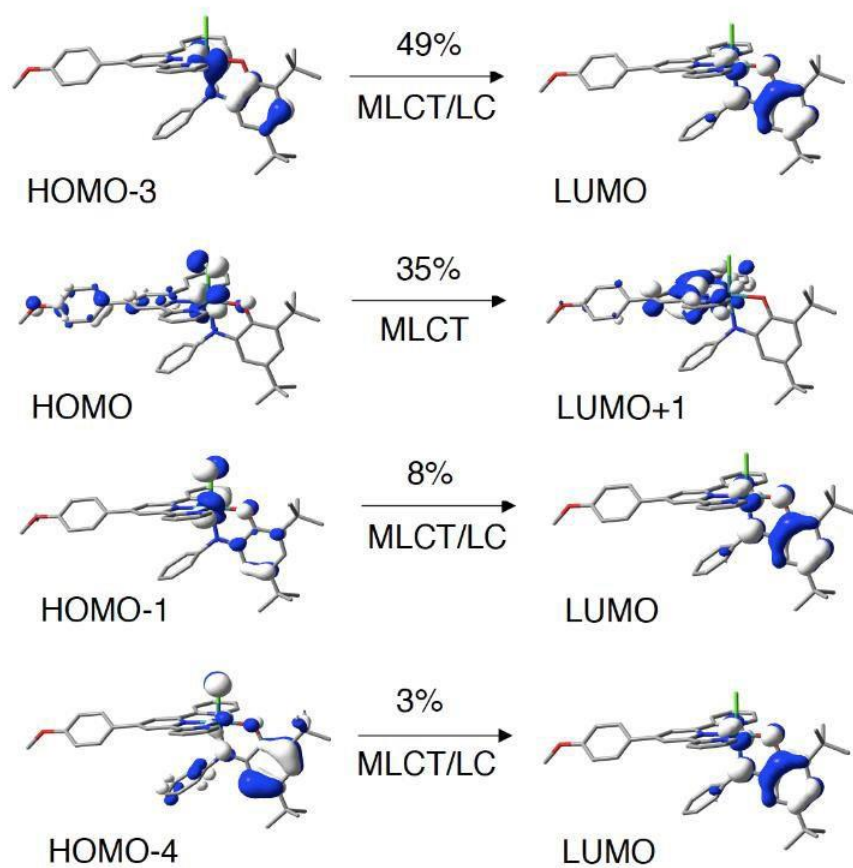


**Table 5:** Calculated Electrochemical data for Ru aminocatechol in dichloromethane (PCM solvent model)

Redox reactions	$E_{1/2}$ (eV) vs Fc/Fc (calculated)	Assignment	$E_{1/2}$ (eV) vs Fc/Fc (Experimental)
$[\text{Ru}(\text{tpy})(\text{O}^{\Delta}\text{N})\text{Cl}]^{2+}$ (D) $\rightarrow$ $[\text{Ru}(\text{tpy})(\text{O}^{\Delta}\text{N})\text{Cl}]^{+}$ (S)	0.95	Ru(IV/III)	0.76
$[\text{Ru}(\text{tpy})(\text{O}^{\Delta}\text{N})\text{Cl}]^{+}$ (S) $\rightarrow$ $[\text{Ru}(\text{tpy})(\text{O}^{\Delta}\text{N})\text{Cl}]^0$ (D)	-0.65	quinone	-0.76
$[\text{Ru}(\text{tpy})(\text{O}^{\Delta}\text{N})\text{Cl}]^0$ (D) $\rightarrow$ $[\text{Ru}(\text{tpy})(\text{O}^{\Delta}\text{N})\text{Cl}]^{1-}$ (S)	-2.07	catechol	-1.60
$[\text{Ru}(\text{tpy})(\text{O}^{\Delta}\text{N})\text{Cl}]^{1-}$ (S) $\rightarrow$ $[\text{Ru}(\text{tpy})(\text{O}^{\Delta}\text{N})\text{Cl}]^{2-}$ (D)	-3.04	terpyridine	-2.22

\*\* S is singlet and D is doublet

**Figure 14:** Natural orbitals of the oxidized and reduced species of  $[\text{Ru}(\text{L}^{\text{terpy}})(\text{L}^2)\text{Cl}]^{\text{PF}_6}$  **1** in dichloromethane

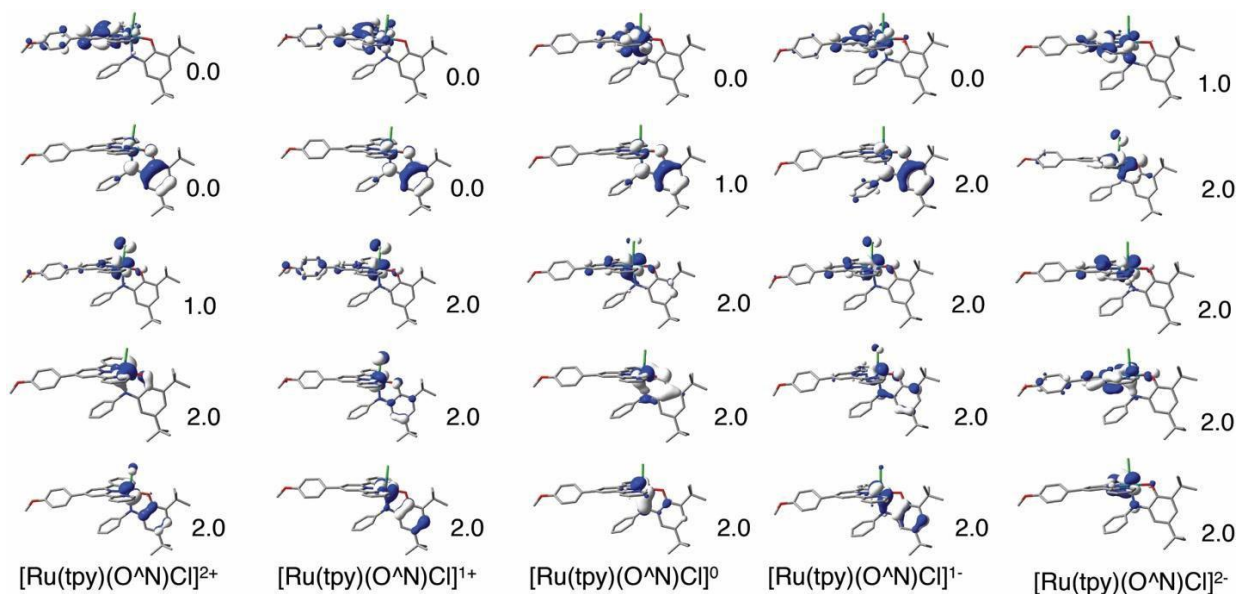


**Figure S15:** I-V characteristics for  $[\text{Ru}(\text{L}^{\text{terpy}})(\text{L}^2)\text{Cl}] \text{PF}_6$  **1** in five devices

